



UKAEA

Preprint



OBSERVATION OF DYNAMIC CHANGES  
IN DENSITY GRADIENTS AND ASSOCIATED  
FLUXES IN THE DITE BOUNDARY LAYER

G. PROUDFOOT  
P. J. HARBOUR

CULHAM LABORATORY  
Abingdon Oxfordshire

1982



---

This document is intended for publication in a journal or at a conference and is made available on the understanding that extracts or references will not be published prior to publication of the original, without the consent of the authors.

Enquiries about copyright and reproduction should be addressed to the Librarian, UKAEA, Culham Laboratory, Abingdon, Oxon. OX14 3DB, England.

## OBSERVATION OF DYNAMIC CHANGES IN DENSITY GRADIENTS AND ASSOCIATED FLUXES IN THE DITE BOUNDARY LAYER

G PROUDFOOT AND P J HARBOUR

Culham Laboratory, Abingdon, Oxon OX14 3DB, UK  
(Euratom/UKAEA Fusion Association)

### ABSTRACT

A Langmuir double probe was used to obtain time-dependent profiles of electron density and temperature in the limiter scrape-off plasma of the DITE tokamak. The line-averaged density  $\bar{n}$  was raised by gas-puffing in conjunction with neutral beam heating, from  $\sim 1$  to  $5 \times 10^{19} \text{ m}^{-3}$  and this was accompanied by (a) an increase in edge density to  $\sim 0.5 \bar{n}$ , (b) substantial variation in the density e-folding scale length in the scrape-off region and (c) a strong increase in the energy and particle fluxes associated with recycling. Modelling of the scrape-off plasma has shown that the recycling became localised close to the limiter at the highest plasma densities. It has been observed that there is a marked difference in the behaviour of the boundary plasma between disruptive and non-disruptive discharge in DITE.

Paper (No.F4) presented at Fifth International Conference on Plasma Surface Interactions in Controlled Fusion Devices, Gatlinburg, Tennessee, 3 May 1982.

May 1982





## 1. Introduction

In our previous work on DITE [1,2] we have reported measurements of boundary layer profiles of electron density and temperature for nominally steady state plasma conditions. Here we describe the use of a Langmuir double probe to investigate the time variation of such profiles for non-steady state conditions in which gas puffing was used in conjunction with neutral injection to raise the line averaged density  $\bar{n}$  to near the density limit in an ungettered torus.

For the discharges investigated, the density at the limiter radius  $n(a)$  ranged between  $0.3$  and  $2.5 \times 10^{19} \text{ m}^{-3}$  and both the parameters  $n(a)/\bar{n}$  and  $\Delta_n$ , the radial scale length for density decay in the limiter shadow, varied strongly with  $n(a)$ . In interpreting these features we use a parallel flow model [3] to relate boundary layer measurements of  $n$  and  $T$  at the probe to their values  $n_\ell$  and  $T_\ell$  on the same magnetic field line at the limiter. The ability of neutrals to penetrate the limiter scrape-off layer has been investigated and changes in their penetration length are related to the above features. Finally the behaviour of the heat and particle balance in the boundary layer is discussed and it is found that the recycling flux can become very large and the power required to ionise it can become comparable with the total discharge power.

## 2. Experimental Configuration and Discharge Conditions

The scrape-off plasma was defined by two poloidal limiters, separated toroidally by  $\phi = 5\pi/8$ : one, a full diaphragm limiter, consisted of a pair of titanium sectors each subtending  $145^\circ$  about the horizontal axis and a pair of overlapping graphite sectors each subtending  $80^\circ$  about the vertical axis; the other, a partial diaphragm, consisted of a similar pair of Ti sectors. The limiter and wall radii were  $0.26$  and  $0.29$  m respectively. The Langmuir probe scanned vertically at the top of the torus at

$R = R(0) = 1.17$  m and was distant  $z_{\ell 1} = 0.44$  m, along a magnetic flux tube, from the carbon sector of the first limiter and  $z_{\ell 2} = 2.32$  m (provided that  $q < 6.5$ ) from the second limiter. The probe was toroidally opposite the gas-puffing port.

Two discharge conditions (A and B) were investigated and the main parameters for these discharges, in deuterium, are given in Table 1 and in Fig.1. For Discharge A during the beam heating phase  $\bar{n}$  increased more rapidly than in the ohmic phase and the rate of increase was fairly constant, indicating that  $1.3 \times 10^{21}$  atom  $s^{-1}$  of deuterium were supplied to the plasma, in agreement with the estimated gas puffing rate. The loop voltage decreased during neutral injection but increased rapidly during the last  $\sim 20$  ms prior to a hard disruption which terminated the discharge. This coincided with a rapid contraction of the radial temperature profile [5] measured by Thomson scattering and electron cyclotron emission. Discharge B was less reproducible, and the density reached a flat top: in this case a hard disruption was not observed.

### 3. Parameters Observed in the Scrape-off Plasma

The Langmuir probe measurements were taken at five radial positions in the scrape-off plasma and averaged over 8 ms intervals. The values of  $n$  and  $T$  have been fitted to an exponential form to determine the associated scale lengths,  $\Delta_n$  and  $\Delta_T$ . The results are plotted in Fig.2 as functions of time. The ratio  $n(a)/\bar{n}$  is also shown. For Discharge A during the ohmic phase, there is evidence for edge cooling when  $n(a)$  was increasing. During beam heating  $T(a)$  increased, almost doubling before reaching a constant  $\sim 8$  eV, and there was a substantial increase in  $n(a)$ . For Discharge B,  $n(a)$  and  $T(a)$  both increased during neutral injection, but the magnitude of  $T(a)$  was higher and that of  $n(a)$  was considerably lower than measured in A. The ratio  $n(a)/\bar{n}$ , shown in Fig.3, was constant ( $\sim 0.25$ ) for

Discharge A at low density, but data from the rest of Discharge A and from B show that  $n(a)/\bar{n}$  increased rapidly with  $n(a)$  indicating a flattening of the density profile, with the scaling  $n(a)/\bar{n} \sim [n(a)]^{3/4}$ . The parameter  $\Delta_n$  also shows a correlation with  $n(a)$  (see Fig.4), decreasing at first from 26 to 10 mm and then increasing in Discharge A to  $\sim 25$  mm at  $n(a) \sim 10^{19} \text{ m}^{-3}$ , beyond which there were no profile data.

#### 4. Transition to Collisional Heat Flow in the Scrape-off Plasma

At the higher scrape-off densities of these experiments the mean free path for Coulomb collisions is small and the flow can then be treated as collisional. Using a one-dimensional fluid model [3] for plasma transport parallel to the magnetic field it can be shown [6] that the plasma temperature  $T_\ell$  at the limiter is related to its value  $T$ , at the probe, by

$$\left(\frac{T_\ell}{T}\right)^{\frac{1}{2}} = \left[1 - \left(\frac{T_\ell}{T}\right)^{7/2}\right] \frac{4\kappa_0}{7\delta_t} \left(\frac{z_{\ell 1} + z_{\ell 2}}{z_{\ell 1} \cdot z_{\ell 2}}\right) \left(\frac{m}{e^3}\right)^{\frac{1}{2}} \frac{T^2}{n(1 + M^2)}. \quad (1)$$

Here  $\kappa_0 T^{5/2}$  is the Spitzer thermal conductivity,  $\delta_t k T_\ell$  is the energy carried to the limiter by each incident ion and its associated electrons,  $m$  is the ion mass,  $M$  the flow Mach number at the probe,  $T$  is measured in eV and  $n$  in  $\text{m}^{-3}$ . The assumptions in this model are (i) that  $T_i = T_e$ , (ii) that heat flows uniformly into a flux tube linking the limiters, is then conducted along the flux tube to be convected through the sheath at each limiter, and (iii) that the density and temperature are related by the momentum equation in the form:

$$nT(1 + M^2) = n_\ell T_\ell (1 + M_\ell^2) = 2n_\ell T_\ell. \quad (2)$$

This equation is for parallel flow along a flux tube, fed by particle sources which do not add momentum to the flow. The sources represent both the volume ionisation and the radial component of the divergence of the particle flux; they need not be uniform, and so Eq.(2) remains valid when recycling is localised around the limiter, provided that there are no associated sources or sinks of momentum.



If numerical values appropriate to DITE are inserted in Eq.(1)

$[\kappa_0 = 31500/(Z \ln \Lambda), Z = 1.25, \ln \Lambda = 10, \delta_t = 9.5 \text{ and } 1 + M^2 \approx 1, \text{ a reasonable assumption at high density}] \text{ we obtain}$

$$\left(\frac{T_\ell}{T}\right)^{\frac{1}{2}} = \left[1 - \left(\frac{T_\ell}{T}\right)^{7/2}\right] 2.61 \times 10^{17} \left(\frac{T^2}{n}\right). \quad (3)$$

The value of  $\delta_t$  used here allows for convection through the sheath and the energy dissipated by ionisation of the recycling gas. It is assumed to be independent of temperature because the temperature dependence of the energy reflection coefficients [7] and of the secondary electron emission coefficients [8,9] are both in the opposite sense to the ionisation losses.

#### 5. Plasma Conditions at the Limiters

Equations (1) and (3) show that  $T_\ell/T$  falls substantially below unity when the Coulomb mean free path  $\lambda_{ee} (\sim T^2/n \ln \Lambda) \lesssim z_{\ell 1}$ . The ratio  $T_\ell(a)/T(a)$  was calculated for both discharges, using Eq.(3). In B the ratio was  $\approx 0.96$  throughout the discharge but in A there was evidence of a transition to collisional heat flow both at  $t \sim 80$  ms and after  $\sim 110$  ms. Figure 5 shows the variation of  $T_\ell(a)/T(a)$  for Discharge A. The corresponding values of  $T_\ell(a)$  fell from  $\sim 12$  to 2 eV and  $n_\ell(a)$ , obtained using Eq.(2) with  $1 + M^2 \approx 1$ , increased by a factor of twenty to  $4 \times 10^{19} \text{ m}^{-3}$ . In the collisional regime,  $T_\ell/T$  scales as  $T^4 n^{-2} \delta_t^{-2}$  so that errors in these parameters limit the conclusions that may be drawn from the data. However, for the particle flux,  $\Gamma_{||,\ell}$  given in Eq.(5) section 7 such errors are less important because this scales as  $n^2 \delta_t T^{-3/2}$  in this regime.



## 6. The Penetration of Neutral Particles through the Scrape-off Plasma

The penetration of neutral particles into and through the scrape-off plasma is dependent both upon their energy and upon the ratio of atomic to molecular deuterium. Both must depend on the source of the neutral species, whether from gas-puffing or from wall or limiter collisions. The smallest penetration distance,  $\lambda_{D_2}$ , is that for molecular deuterium (taken at 0.025 eV) undergoing ionisation or dissociation by electron impact [10]. Some of the resulting species are not charged and a proportion will penetrate the scrape-off plasma, but if  $\lambda_{D_2} \gg \Delta_n$  we may conclude that the scrape-off particle flow can only be fed by radial diffusion from the confinement region and that this is unlikely to vary toroidally. In these circumstances the parallel flow velocity is likely to be high. If  $\lambda_{D_2} \lesssim \Delta_n$  then ionisation sources in the scrape-off plasma are significant and recycling of  $D_2$  can be localised at the limiter. Atoms can penetrate to a greater distance and this is characterised by  $\lambda_o$ , a mean free path for the ionisation of deuterium atoms which are diffusing via charge exchange collisions [11], given by

$$\lambda_o = v_o / n [3\langle\sigma v\rangle_{cx} \langle\sigma v\rangle_i]^{1/2} . \quad (4)$$

These mean free paths have been calculated for conditions near the probe and limiter at  $r=a$  and are shown in Fig.6. Only in the early phases of Discharge A was  $\lambda_{D_2} \gg \Delta_n$  and so only here was the scrape-off flow predominantly fed by radial diffusion. This might relate to the minimum in  $\Delta_n$  (Fig.4) and to the relatively constant value of  $n(a)/\bar{n}$  observed only during this phase of Discharge A. The fact that  $\lambda_o \gg \Delta_n$  for both discharges indicates that atoms recycled from the limiter might readily penetrate the scrape-off plasma if emitted radially inwards but those travelling outwards may be recycled locally, either before or after collisions with the walls. Also shown in Fig.6 is  $\lambda_{cx}$ , the charge exchange mean free path [10] for deuterium atoms, assumed to be at the local plasma temperature. In general,  $\lambda_{cx} > \Delta_n$  and

charge exchange is only important if it affects the flow momentum, as might have occurred in the last  $\sim 20$  ms of Discharge A where  $\lambda_{cx,l} \ll \Delta_n$  and  $\lambda_{D2,l}$  was increasing.

#### 7. Heat and Particle Balance in the Boundary Plasma

The fluxes to the limiters were evaluated at  $r = a$  using, for the particle flux,

$$\Gamma_{||,l} = n_l v_l = n_l (2kT_l/m)^{1/2}, \quad (5)$$

and, for the heat flux,

$$q_{||,l} = \Gamma_{||,l} \delta_t kT_l. \quad (6)$$

These values can also be used to calculate the total flow of particles and energy to the limiters, making the assumption that the flow to all limiters is identical, ie, ignoring the lack of toroidal symmetry in the geometry of the limiters and gas-puffing port. For both Discharges A and B, whether in the ohmic or beam heating phase, the estimated total power to the limiters was a small fraction ( $\sim 10$ -15%) of the total power available and the overall particle confinement time is estimated to have been fairly constant,  $\sim 11$ -12 ms.

The values of  $q_{||,l}$  and  $\Gamma_{||,l}$  obtained from Eqs.(5) and (6) are plotted in Fig.7. The magnitude of  $\Gamma_{||,l}$  for Discharge A was much larger than for B, and increased roughly exponentially with time to a final value prior to the disruption of  $6.2 \times 10^{23} \text{ m}^{-2} \text{ s}^{-1}$ . The corresponding total particle flow to the limiters is  $7 \times 10^{22} \text{ s}^{-1}$ . This flow substantially exceeds both the estimated gas feed rate of  $1.3 \times 10^{21} \text{ s}^{-1}$  and the estimated radial flow of particles across the limiter radius of  $1 \times 10^{22} \text{ s}^{-1}$  (based on  $\Gamma_{\perp} \approx D_{\perp} n(a)/\Delta_n$  with  $D_{\perp} \approx 1 \text{ m}^2 \text{ s}^{-1}$ ). The magnitude of  $q_{||,l}$  was less variable. A minimum is present in Discharge A and this coincides with the minimum in  $\Delta_n$ .

Although the total conducted power to the limiters was not large, the



power associated with the ionisation of recycled particles is very large indeed and exceeds the power flow to the limiters when  $\bar{n} \gtrsim 4 \times 10^{19} \text{ m}^{-3}$ . The value is almost 500 kW for  $7 \times 10^{22}$  atoms per second (assuming 40 eV per ionisation).

## 8. Conclusions

Time-dependent measurements of plasma parameters in the limiter scrape-off plasma have demonstrated the importance of collisional processes in the boundary region of high density tokamak discharges. As the density increases the location of particle recycling tends to be in the immediate vicinity of the limiter. The density scale length,  $\Delta_n$ , correlates with  $n(a)$ , exhibiting a minimum which may be related to a low parallel heat flow in the scrape-off layer and also to a high Mach number when  $\lambda_{D2} \gg \Delta_n$ . The ratio  $n(a)/\bar{n}$  apparently scales with the three-quarters power of  $n(a)$ , indicating a flattening of the density profile at high density, a feature widely predicted because of the reduced penetration of recycling neutral particles, but not generally observed in tokamaks. The highest observed value of  $n(a)/\bar{n}$  was  $\approx 0.5$ , measured when  $n(a) \approx 2.5 \times 10^{19} \text{ m}^{-3}$ , but if the correlation with  $n(a)$  is extrapolated, we find  $n(a) = \bar{n}$  at  $\bar{n} \approx 6.3 \times 10^{19} \text{ m}^{-3}$ , a value which might have been reached just before  $t = 150 \text{ ms}$  (see Fig.2) but for the terminal disruption. The cause of the disruption is uncertain, but immediately prior to it the following events were occurring:

- i. The edge density was approaching the line averaged density.
- ii. The particle flow associated with recycling may have been sufficient to trigger an instability in the radial particle transport.
- iii. The energy flow associated with recycling may have led to the observed cooling [5] in the outer part of the discharge and so to rapid constriction of the current profile.

Some of these conclusions are based on a model which predicts toroidal variations but these have not yet been verified experimentally.

#### Acknowledgment

The authors thank the DITE operating team and also Dr J Hugill and Mr M F A Harrison for valuable discussions.

#### References

- [1] G Proudfoot and P J Harbour, J.Nucl.Mat. 93 and 94 (1980) 413.
- [2] P J Harbour and G Proudfoot, Proc.IAEA Tech.Committee on Divertors and Impurity Control (IPP 1981) p.45.
- [3] M F A Harrison, P J Harbour and E S Hotston, submitted to Nucl.Fusion 1982 (Culham Laboratory preprint CLM-P668).
- [4] G M McCracken, private communication.
- [5] J Hugill, private communication.
- [6] P J Harbour, to be published.
- [7] W Eckstein and H Verbeek, IPP 9/32 (Aug.1979).
- [8] P J Harbour and M F A Harrison, J.Nucl.Mat. 76 and 77 (1978) 513.
- [9] M-C Saussez-Hublet and P J Harbour, Culham Laboratory Report CLM-R208 (June 1980).
- [10] M F A Harrison in Applied Atomic Collision Physics, Vol.II, to be published by Academic Press.
- [11] P J Harbour in Section 11 of Culham Laboratory Report CLM-R211 (Aug.1981).

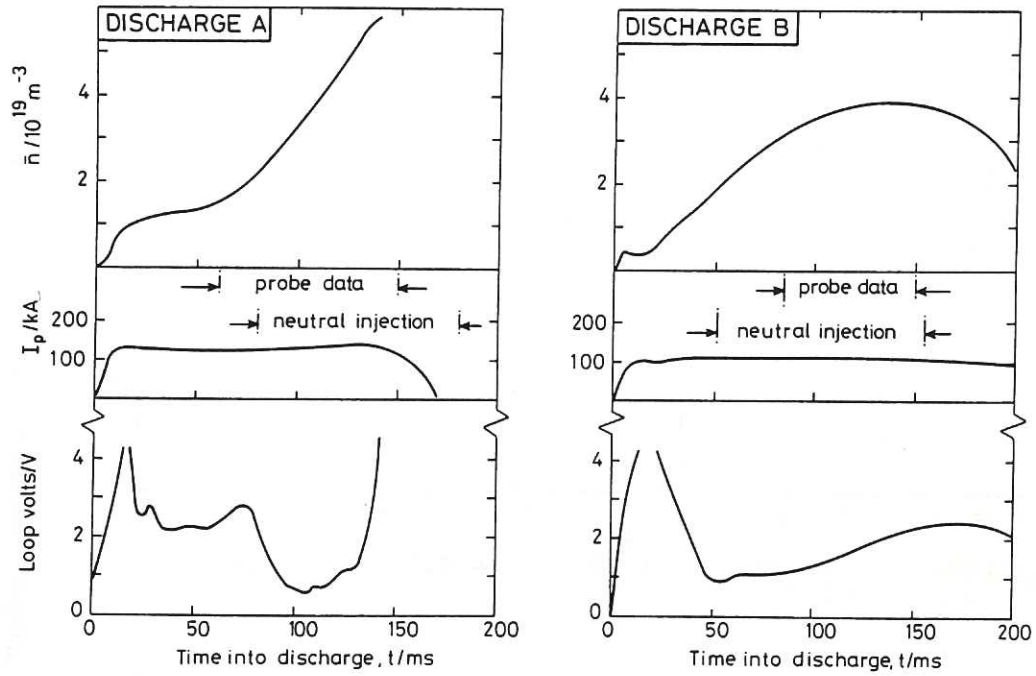


Table 1Discharge Parameters

Discharge	A	B
Plasma current, $I_p$ /kA	130	115
Toroidal field, $B_\phi$ /T	2.7	1.36
Safety factor, $q(a)$	6	3.4
NI Power/MW	1	0.5
Energy of H-Beam/keV	24	24
Energy to partial diaphragm limiters/kJ [4]	-	11
Hard disruption?	Yes	No







**Fig.1 Time variation of plasma parameters for the two DITE discharge conditions of Table 1. Discharge A terminated disruptively at  $t = 140 \pm 10\text{ms}$  but, during the period when probe data were recorded, the plasma position was maintained.**

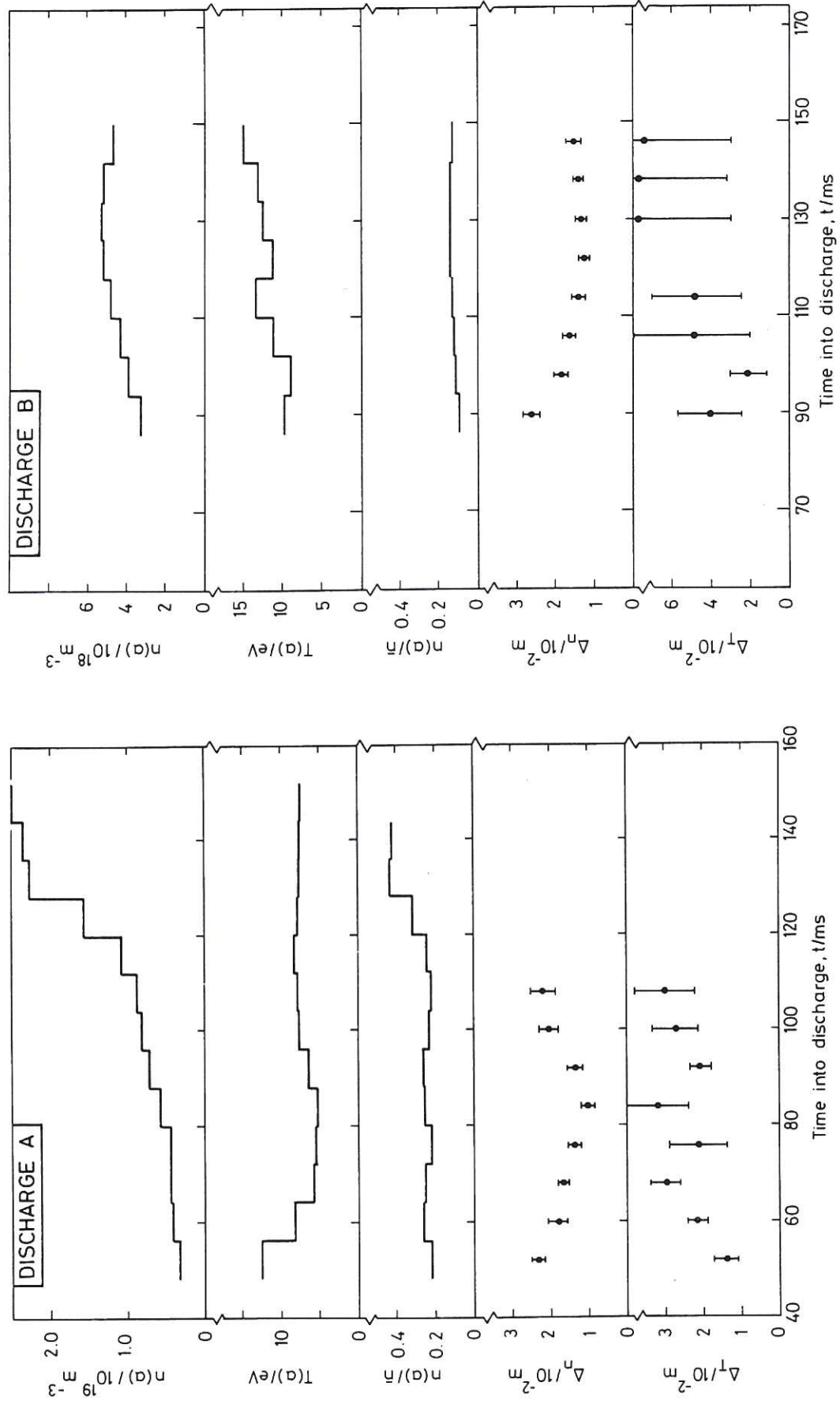


Fig.2 The variation of scrape-off parameters, averaged over 8 ms, evaluated at the limiter radius ( $a = 0.26\text{ m}$ ). Error bars show statistical errors and those associated with shot-by-shot averaging. At  $t > 130\text{ ms}$ , data were selected from discharges with a later disruption time.



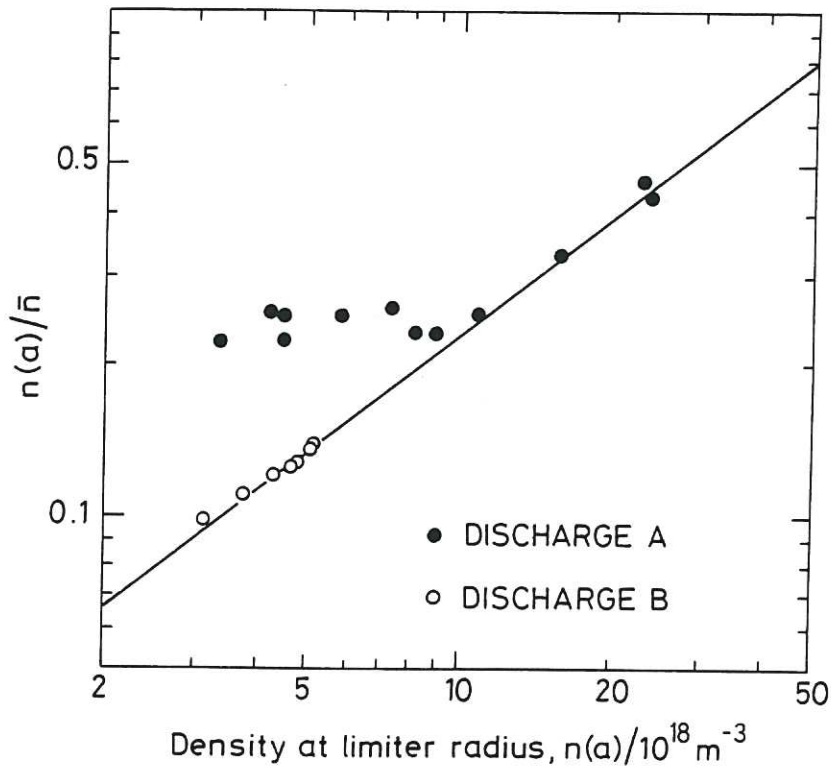


Fig.3 A correlation between the ratio  $n(a)/\bar{n}$  and  $n(a)$ . The solid line is fitted to the data.

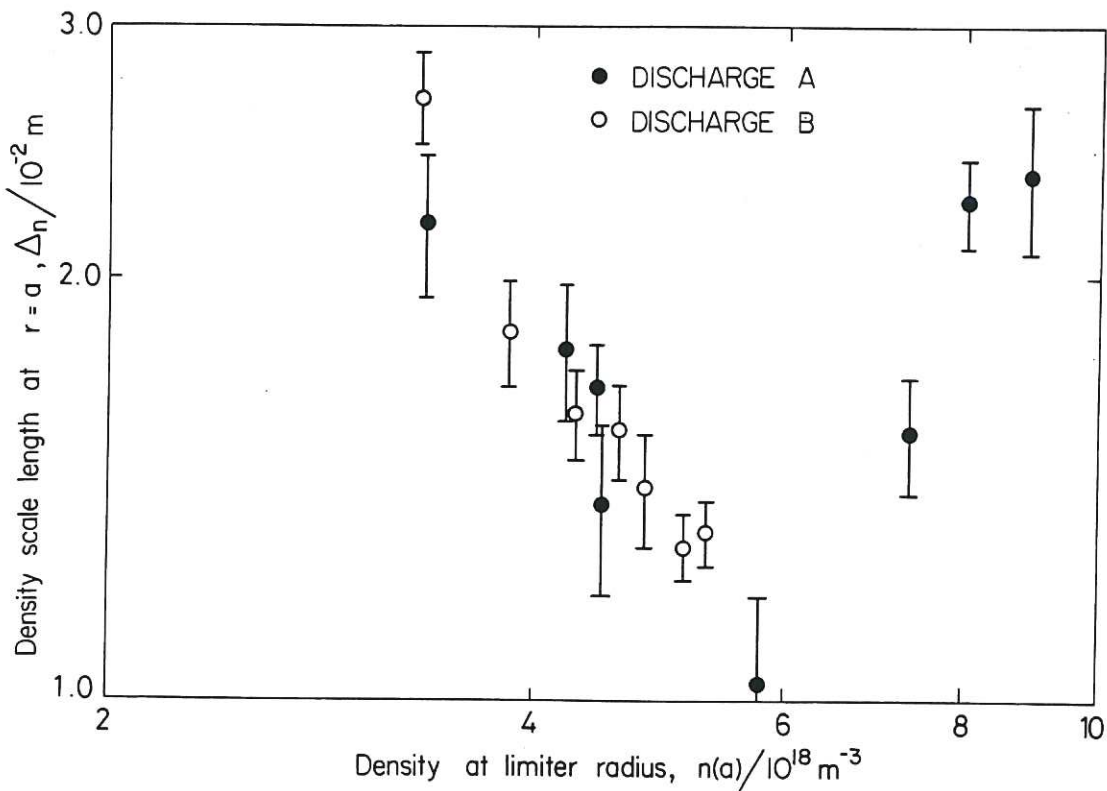


Fig.4 The variation of density scale length at the limiter,  $\Delta_n$ , with density at the limiter radius  $n(a)$ .

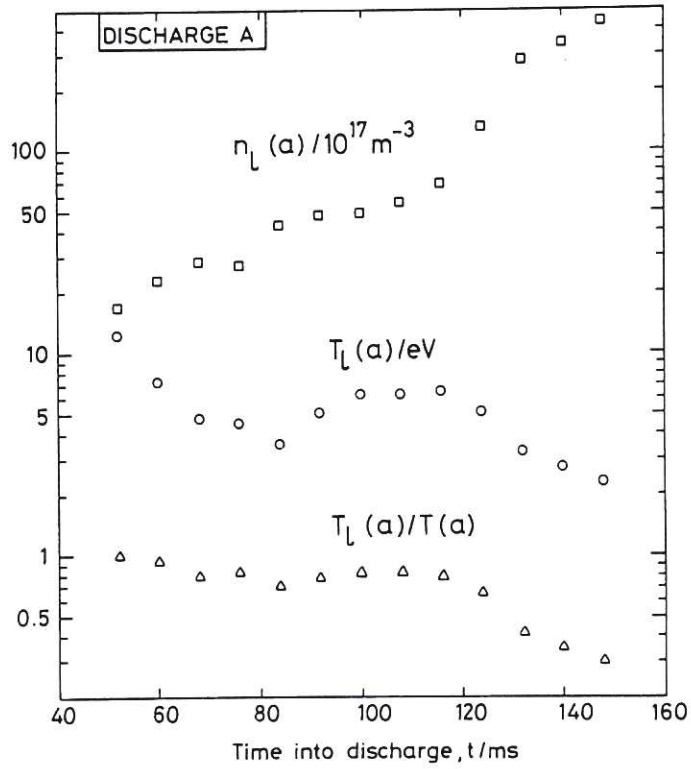


Fig.5 Time-variation of scrape-off parameters  $n_L$ ,  $T_L$  at the limiter (at  $r = a$ ) obtained from the probe data  $n(a)$ ,  $T(a)$  by the use of Eqs.(2) and (3).

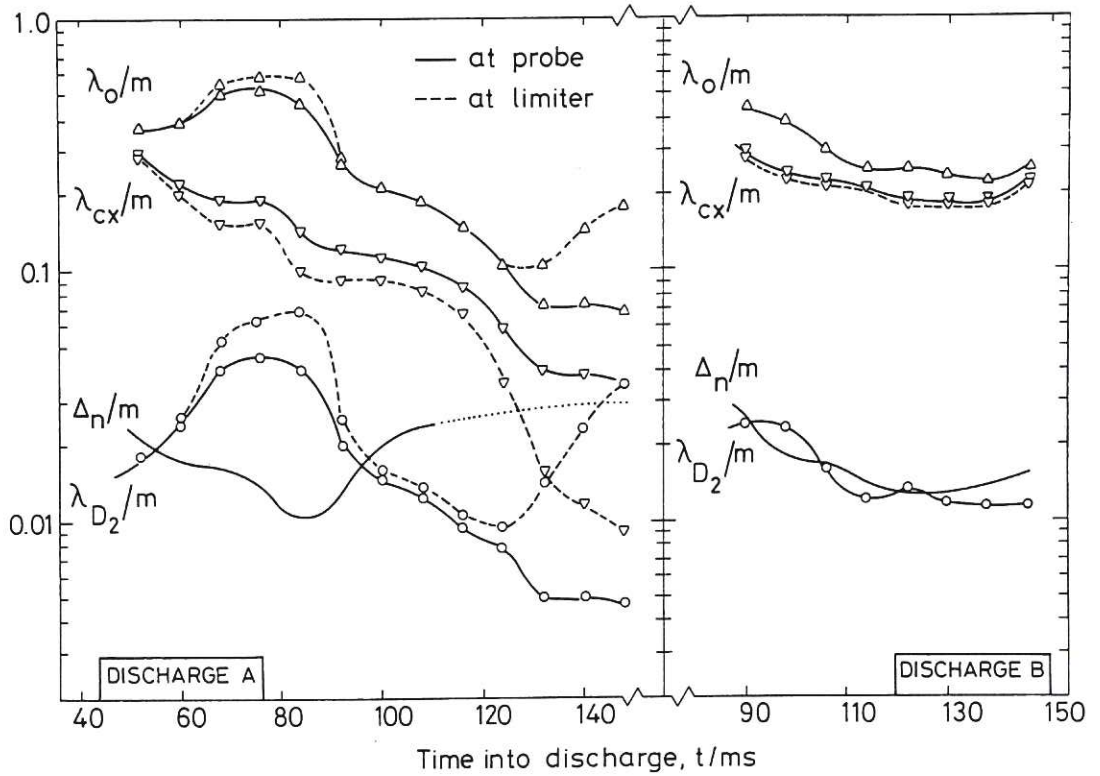


Fig.6 Time-variation of mean free paths for recycling and gas puffed neutral particles, based on the probe data  $n(a)$  and  $T(a)$  and on the values at the limiter,  $2n_L(a)$  and  $T_L(a)$ .



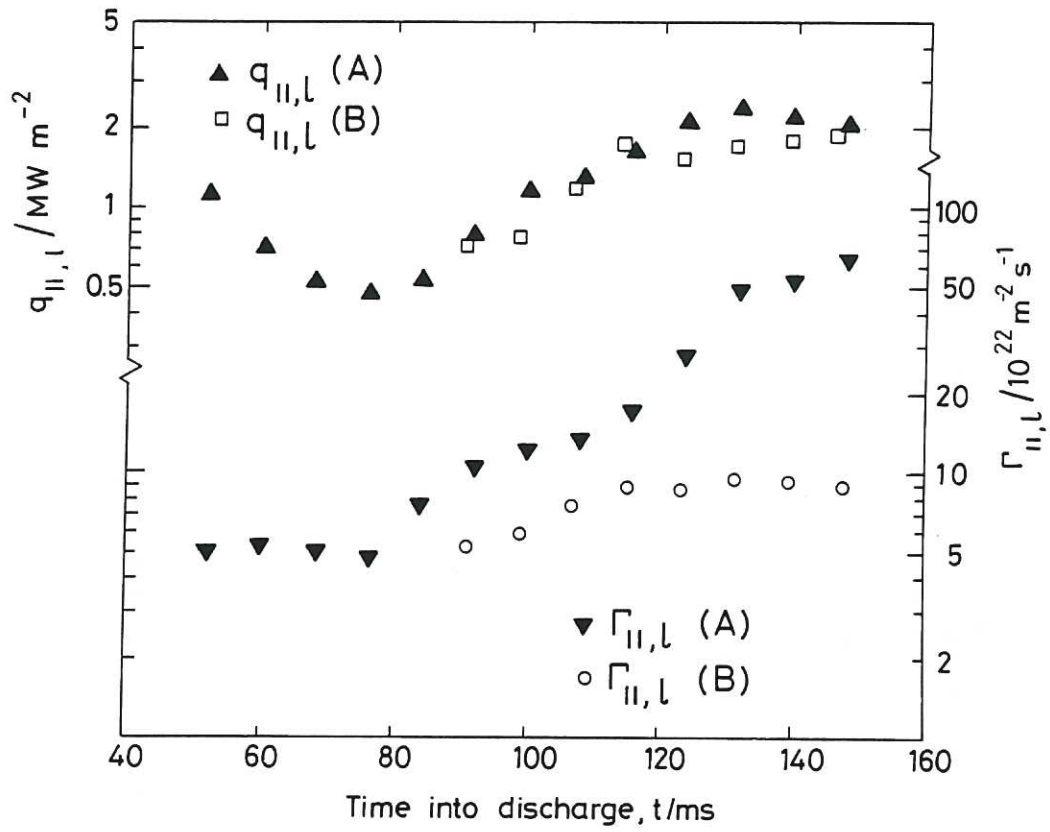


Fig.7 Time-variation of the parallel flux of particles and energy to the limiter, evaluated using Eqs.(5) and (6) at  $r = a$ . The value of  $q_{||,l}$  in Discharge B may also be compared with a value of  $1.4 \text{ MW m}^{-2}$ , based on calorimetric measurements [4] of the total energy deposited on a pair of limiters during the discharge.



